Received: 6 June 2024 | Revised: 16 July 2024 | Accepted: 30 July 2024

DOI: 10.1002/app.56127

RESEARCH ARTICLE

Applied Polymer SCIENCE WILEY

Triazole-, piperazine-, and DOPO-containing eugenol-based reactive flame retardant for unsaturated polyester resin

Ozge Ozukanar[1] | **Gokhan Sagdic**[1] | **Emrah Çakmakçı**[2] | **Fadime Karaer Özmen**[3] | **Mustafa E. Üreyen**[4,5] | **Ufuk Saim Gunay**[1] | **Hakan Durmaz**[1] | **Volkan Kumbaraci**[1]

[1]Department of Chemistry, Istanbul Technical University, Istanbul, Türkiye

[2]Department of Chemistry, Marmara University, Istanbul, Türkiye

[3]Environmental Engineering Department, Engineering Faculty, Eskisehir Technical University, Eskisehir, Türkiye

[4]Department of Fashion and Textile Design, Faculty of Architecture and Design, Eskisehir Technical University, Eskisehir, Türkiye

[5]Advanced Technologies Research Centre (ITAM), Eskisehir Technical University, Eskisehir, Türkiye

Correspondence
Emrah Çakmakçı, Department of Chemistry, Marmara University, Istanbul 34722, Türkiye.
Email: emrah.cakmakci@marmara.edu.tr

Volkan Kumbaraci, Department of Chemistry, Istanbul Technical University, Istanbul 34722, Türkiye.
Email: kumbaracii@itu.edu.tr

Funding information
Scientific Research Projects Department of Istanbul Technical University

Abstract

The flammability of unsaturated polyester resins (UPRs) limits their applications. Herein, a reactive P- and N-containing flame retardant (DPET) having triazole and piperazine rings is reported. The 9,10-Dihydro-9-oxa-10-phosphaphenanthrene 10-oxide (DOPO) was used to introduce P atoms, and eugenol was used to import reactive double bonds to DPET. Different ratios of DPET were mixed with a commercial UPR and the thermal, mechanical, optical, and flame retardancy properties were measured. The addition of 15% of DPET into neat UPR led to a decrease in the water contact angle from 70° ± 2 to 61° ± 2. The gel content values of the UPRs were found to change between 97.5% and 89%. The optical properties of the UPR were adversely affected by the incorporation of DPET. The modulus of the DPET-containing UPRs increased with increasing amount of DPET and 15% of DPET-containing UPR displayed a modulus value of 1784 ± 86 MPa. When 15% DPET was added to neat UPR, char yields were increased (from 5.6% to 16.6%). Limiting oxygen index (LOI) values increased with increasing amounts of DPET and reached up to 23.4%. Micro cone calorimeter (MCC) test results showed up to a 20.5% reduction in the peak heat release rate (PHRR) of the UPR when 15% DPET was added.

KEYWORDS
flame retardance, radical polymerization, resins, thermal properties, thermosets

1 | INTRODUCTION

Thermosets are highly cross-linked polymer networks that are infusible.[1] Some of the important members of the thermoset family are unsaturated polyester resins (UPRs), epoxy resins, phenolic resins, cyanate resins, benzoxazines, and so forth. Among them, UPRs are extensively used in maritime, building and construction, electronics, automotive, and aerospace industries as a matrix material for glass fiber composites, as casting resins, or as coatings due to their low-cost, low density, outstanding mechanical properties, and chemical resistance.[2–6]

UPRs are generally prepared from the condensation reaction of aromatic dicarboxylic acids (or acid anhydrides), various diols, and maleic acid or maleic anhydride.[7] The obtained unsaturated polyester is then

dissolved in styrene, a reactive diluent, to reduce viscosity. The resulting resins are often cured according to the free-radical mechanism at high temperatures with the aid of thermal initiators or at room temperature via thermal initiators such as peroxides and accelerators (promoters) such as cobalt octoate.

Despite their exceptional properties and wide use, UPRs suffer from high flammability, resulting from their chemical composition and molecular structure.[8,9] Both the polyester and the polystyrene segments easily undergo random bond cleavages, and simultaneously, polystyrene chains depolymerize to highly flammable styrene monomer at high temperatures.[10] Thus, the inherent flammability of UPRs limits their applications. Recently, various flame retardants (FRs) have been suggested in the literature to overcome this poor resistance of UPRs such as adenosine triphosphate/imidazole/graphite,[11] DOPO-containing polymers and compound,[12,13] phosphazene-modified metal organic frameworks,[14] benzimidazole-modified ammonium polyphosphate (APP),[15] cyanuric chloride/DOPO derivatives,[16] and zinc /triazole/phosphate or copper/melamine/phosphate compounds.[17]

Halogen- and P-containing compounds are the most prominent FRs for polymers; however, the former ones have toxic effects and most of the halogenated FRs are either banned or have restricted use in plastics. Thus, researchers' attention has shifted towards P-containing FRs. These halogen-free phosphorous FRs can be classified into two groups; the additive types and the reactive ones. For instance, APP is a widely used FR additive.[18] Tough APP is an effective FR, often it must be added at high loadings to achieve a good level of fire resistance, which leads to poor mechanical properties.[18–22] Besides, APP is not hydrolytically stable, decomposes over time, and migrates from the polymer matrix, resulting in the reduction of flame retardancy. To overcome the issues associated with the use of non-reactive additive types of FRs, in recent years, P-containing reactive FRs have gained much interest.[23–29]

It is known from the literature that FRs having elements such as N, B, or Si, in addition to P in their chemical structures, display better FR properties.[30–33] The P–N synergistic effect is well-known and widely utilized for the design and synthesis of FRs. Upon combustion, phosphorous species often work in the condensed phase and catalyze the formation of dense carbonaceous char, while nitrogen-containing organic molecules release gases like ammonia which dilutes the oxygen concentration in the gas phase, thereby contributing to the flame retardancy.[34–37] Besides, as the carbonaceous char forms, the released gases lead to the expansion of this char residue, and a foam-like structure forms. These types of FRs are known as intumescent FRs and are highly efficient. While urea and melamine are among the most preferred N-containing FR additives, researchers have designed several phosphorous FRs having N-containing heterocycles such as triazole,[35] piperazine,[37] piperidine,[38] imidazole,[39] and so forth, to exploit the P–N synergism for various thermosets.

The 9,10-Dihydro-9-oxa-10-phosphaphenanthrene 10-oxide (DOPO) is a popular FR and it was previously used as a starting compound for the synthesis of reactive FRs for UPRs.[39–43] For instance, Bai et al. synthesized a DOPO-based diacrylate monomer (ODOPB-AC) and added it to a commercial UPR in different ratios.[40] Twenty percentage ODOPB-AC-containing thermosets displayed a limiting oxygen index (LOI) value of 28%. The UL-94 test was not performed in the work of Bai et al., and the absence of nitrogen in the structure of ODOPB-AC would have influenced the UL-94 test. Lin et al. prepared a UPR by using a DOPO-derived monoacrylate monomer (DHP)[41] Thermosets containing 20% DHP displayed a LOI value of 29%. However, it must be noted that the LOI value for the neat UPR in the work of Lin et al., was reported to be 23% which is a high value for an UPR resin. Therefore, it must be considered that the LOI was increased to 29% from 23%. In another work, Cao et al. synthesized a reactive bi-DOPO derivative, namely TDCAA-DOPO.[42] When TDCAA-DOPO was incorporated into UPR, the LOI values and the mechanical properties were enhanced. It must be noted that the use of bi-DOPO-containing reactive FRs for UPRs is rare. To our knowledge, there are also a few examples that describe the synthesis of DOPO-based, P- and N-containing reactive FRs for UPRs.[43–45] Huo et al. reacted DOPO with triallyl isocyanurate to prepare a triazine-trione group-containing reactive FR (DT)[45] P- and N-containing DT was added to UPR at different ratios and the LOI value increased to 29.8% (30% DT-containing formulation) from 19% (neat UPR).

Herein, we report the synthesis of a novel reactive FR having a bi-DOPO structure as well as triazole and piperazine rings. To introduce reactive groups to the newly synthesized FR compound, we used a bio-based monomer, eugenol. Eugenol can be extracted from clove oil and also can be obtained from the depolymerization of lignin.[36,37] The use of renewable feedstock is important for sustainable and eco-friendly FR development.[46,47] Besides, a metal-free azide-alkyne click reaction was applied to synthesize the FR compound. Recently, the studies demonstrating the successful use of click reactions for FR synthesis have started to pile up.[28,48,49]

The originality of this study stems from the use of metal-free click reactions, the presence of a bi-DOPO structure, and the combination of two N-containing rings; triazole and piperazine. The use of modern metal-free azide-alkyne click reactions for the synthesis of FRs is an intriguing and effective approach and leads to the formation of triazole groups. Besides, in this work we

used a bio-based building block, eugenol, to introduce reactive groups. With these aspects, the compound synthesized herein is innovative and has a different perspective compared to the existing literature on FRs for UPRs. To our knowledge, an FR compound that combines triazole and piperazine groups was not previously synthesized in the literature for UPRs. Besides, the use of metal-free click reaction for an FR synthesis is not commonly practiced and we believe it is an interesting strategy that needs to be explored more. We also believe this is the first work in the literature that reports the utilization of metal-free click reaction for the synthesis of an FR compound to be used in UPRs. We concur that our work closes a gap in the literature, provides a significant contribution, and offers a fresh viewpoint on the synthesis and design of FRs. The nitrogen-rich DOPO-based FR described herein was characterized by using nuclear magnetic resonance spectroscopy (NMR) and Fourier-transform infrared spectroscopy (FTIR) spectroscopies. Different ratios of this FR (5%, 10%, 15%) were added to a commercial UPR and the UPRs were thermally cured. The mechanical, thermal, optical, and FR properties of the UPRs were measured.

2 | EXPERIMENTAL

2.1 | Materials

Anhydrous sodium sulfate, potassium carbonate (K_2CO_3), triethyl amine (Et_3N), sodium chloride, sodium hydroxide (NaOH), tetrabutylammonium bromide (TBAB), piperazine, eugenol, epichlorohydrin (ECH), dichloromethane (DCM), ethyl acetate, hexane, chloroform ($CHCl_3$), thionyl chloride ($SOCl_2$), N,N-dimethylformamide (DMF), propiolic acid, paraformaldehyde, para-toluene sulfonic acid (p-TSA), and sodium azide were purchased from Sigma Aldrich. The 9,10-Dihydro-9-oxa-10-phosphaphenanthrene 10-oxide was purchased from TCI. All solvents were of HPLC or ACS grade. The 1 (EECH) and 2 (BEECH) were prepared according to a literature study.[37] The UPR used in this work is composed of isophthalic acid, maleic anhydride, glycol, and 35%–40% styrene and it was purchased from a local company.

2.2 | Characterization methods

Proton nuclear magnetic resonance (^{1}H-NMR) measurements were recorded with $CDCl_3$ using an Agilent VNMRS (500 MHz) instrument. The carbon nuclear magnetic resonance (^{13}C-NMR) spectra were recorded at Agilent VNMRS 125 MHz. FTIR spectra were recorded on an Agilent Technologies Cary 630 FTIR instrument over the range of 4000–500 cm^{-1}. Ultra Performance Liquid Chromatography measurements (UPLC-QTof) were performed by using a Waters (Acquity H Class Plus) UPLC instrument equipped with Vion IMS QTof. Thermogravimetric analyses (TGA) of the photocured films were performed by using a PerkinElmer thermogravimetric analyzer (Pyris 1 TGA model). Samples were run from 30 to 600°C with a heating rate of 10°C/min under a nitrogen atmosphere. The flame retardancy of the UPRs was assessed by measuring the LOI, UL-94 test, and micro cone calorimeter (MCC) test was conducted for further evaluation. The LOI values were measured on an oxygen index meter (FTT, Fire Testing Technology). According to ASTM D2863-00 the specimens were used for LOI with 120 mm × 10 mm × 4 mm. FAA MCC was used to investigate the combustion of the composites. In this system, about 3 mg samples of the composites were heated to 900°C at a heating rate of 1°C/s and in a stream of nitrogen flowing at 80 mL/min. The heat release rate (HRR), heat release capacity (HRC), and total heat release (THR) were obtained from MCC measurements in the micro-scale test. UL-94 was performed according to ASTM D3801-00. The samples sized 130 mm × 12.5 mm × 4 mm were placed over the burner for 10 s.

Fire effluent was determined with simultaneous TGA–FTIR evolved gas analysis for all samples under the following conditions 600°C, 30°C/min heating rate, 100 mL/min nitrogen gas a flow rate in the TGA (TA Instrument, SDTQ600, USA), and combustion products were determined with FTIR (Agilent Carry 600, USA) simultaneously. Gel contents were determined by immersing the pre-weighted samples (~0.5 g) in xylene (20 mL) for 24 h. The insoluble gel fraction was dried in a vacuum oven at 100°C to constant weight and the gel percentage was calculated. The wettability characteristics of the coatings were performed on a Kruss (Easy Drop DSA-2) tensiometer. The contact angles (h) were measured using sessile drop test method in which drops were created using a syringe. Measurements were made using 3–5 μL of distilled water. For each sample, at least five measurements were made, and the average value was reported. Scanning electron microscopy with an energy-dispersive x-ray analytical system (Zeiss EVO LS 10, SEM–EDX) was used to characterize the microstructure of the char residues.

2.3 | Synthesis of 1,4-bis(3-(4-allyl-2-methoxyphenoxy)-2-azidopropyl) piperazine (3, BEECHDA)

Into a 100 mL of two-necked round-bottom flask, 2 (1 eq., 1.80 g, 3.42 mmol) was added and dissolved in 30 mL of $CHCl_3$. The solution was cooled to 0°C using an

ice bath, and then $SOCl_2$ (2.5 eq., 0.62 mL, 8.54 mmol) diluted with 5 mL of DCM was added to the solution dropwise under nitrogen. After the addition was completed, the mixture was stirred for 1 h. Excess solvent was evaporated, then 10 mL DMF and sodium azide (4 eq., 0.90 g, 13.70 mmol) were added to the flask. The reaction mixture was stirred at room temperature overnight. The progress of the reaction was monitored by FTIR. When the reaction was complete, the mixture was washed with K_2CO_3 solution, dried with Na_2SO_4, filtered, and the excess solvent was evaporated. Brown viscous liquid was obtained with 84% (1.66 g) yield and used without further purification in the next step.

^{1}H NMR ($CDCl_3$, δ) 6.84–6.81 (m, 2H, Ar—H), 6.75–6.69 (m, 4H, Ar—H), 6.01–5.92 (m, 2H, C═CH), 5.12–5.05 (m, 4H, C=CH_2), 4.16–4.12 (m, 2H, OCH_2), 4.02–3.97 (m, 2H, OCH_2), 3.83 (s, 6H, OCH_3), 3.62–3.57 (m, 2H, NH_2), 3.51–3.46 (m, 2H, NH_2), 3.37–3.32 (4H, Ph—CH_2), 3.14–3.08 (2H, CH—N_3), 2.89–2.69 (m, 8H, NCH_2CH_2N).

^{13}C NMR ($CDCl_3$, δ) 149.87, 146.41, 137.56, 133.87, 120.53, 115.70, 114.54, 112.66, 72.43, 69.34, 66.89, 62.99, 55.90, 49.80, 49.16, 39.83.

FTIR (cm^{-1}): 2991, 2096, 1669, 1509, 1448, 1418, 1213, 1138, 1030, 915.

2.4 | Synthesis of (6-oxidodibenzo[c,e][1,2]oxaphosphinin-6-yl)methyl propiolate (5, DOPO-propiolate)

The 5 was prepared in two steps. First, 4 was prepared by reacting DOPO with paraformaldehyde according to the literature.[50–52] Then, to a 100 mL of round-bottom flask equipped with a magnetic stir bar, 4 (2.40 g, 9.75 mmol), propiolic acid (3.63 mL, 58.49 mmol), p-TSA (0.927 g, 4.87 mmol), and 20 mL benzene were added. After that, the flask was attached to a Dean–Stark apparatus and left to stir in the reflux overnight. Next, benzene was evaporated, and the mixture was diluted with 100 mL of DCM and extracted with 100 mL of distilled water three times. The organic layers were dried over anhydrous Na_2SO_4, filtered, and evaporated to dryness to give 5 as a pale brown solid. The crude product was washed with small amounts of cold methanol to give a white solid. Yield: 2.74 g (94%).

^{1}H NMR ($CDCl_3$, δ) 8.04–7.26 (m, 8H, Ar—H), 4.84–4.74 (m, 2H, P═OCH_2), 2.82 (s, 1H, C≡CH).

^{13}C NMR ($CDCl_3$, δ) 151.23, 151.03, 149.27, 136.57, 134.28, 130.86, 130.26, 128.83, 128.07, 124.89, 123.69, 121.75, 121.36, 120.75, 120.24, 73.04, 61.16, 60.22.

^{31}P NMR ($CDCl_3$, δ) 26.33.

FTIR (cm^{-1}): 3155, 2105, 1712, 1595, 1476, 1425, 1312, 1193, 936, 853, 803, 740, 510.

ESI-MS, m/z $C_{16}H_{11}O_4P$ calculated: 298.0395; Found: 299.0468 $[M + H]^+$.

2.5 | Synthesis of bis((6-oxido-6H-dibenzo[c,e][1,2]oxaphosphinin-6-yl) methyl) 1,1′-(piperazine-1,4-diylbis (1-(4-allyl-2-methoxyphenoxy)propane-3,2-diyl))bis(1H-1,2,3-triazole-4-carboxylate) (6, DPET)

The 3 and 5 were coupled via a metal-free azide-alkyne click reaction. To a 25 mL Schlenk tube equipped with a magnetic stir bar, 5 (2.3 eq., 1.19 g, 4.39 mmol) and 3 (1 eq., 1.10 g, 1.91 mmol) were added and dissolved in 10 mL of $CHCl_3$. After two freeze-pump-thaw cycles, the tube was placed in an oil bath stirred at 80°C for 24 h. Afterward, excess $CHCl_3$ was evaporated, and the solution was precipitated into hexane. This procedure was repeated two times. Finally, the excess solvent was decanted and the product was obtained as a pale yellow oil. Yield: 1.64 g (73.3%).

^{1}H NMR ($CDCl_3$, δ) 8.04–7.21 (m, 24H, Ar—H), 6.86–6.67 (m, 6H, Ar—H), 5.95 (m, 2H, C═CH), 5.11–5.04 (m, 4H, C═CH_2), 4.96–4.51 (m, 8H, PCH_2 + OCH_2), 4.11–3.89 (m, 4H, NCH_2), 3.87–3.77 (m, 6H, OCH_3), 3.35 (4H, Ph—CH_2), 2.95–2.25 (m, 10H, NCH_2CH_2N + CH—N_3).

^{13}C NMR ($CDCl_3$, δ) 159.11, 149.70, 145.79, 143.92, 137.81, 137.38, 134.21, 131.18, 130.70, 128.85, 124.99, 124.58, 123.64, 121.78, 121.15, 120.62, 120.30, 115.90, 115.51, 114.97, 114.27, 112.51, 113.13, 73.05, 68.48, 66.53, 63.20, 61.17, 60.79, 60.23, 59.86, 55.86, 55.66, 49.53, 48.67, 39.85, 39.83, 29.69.

FTIR (cm^{-1}): 3304, 2924, 2098, 1709, 1593, 1511, 1448, 1431, 1358, 1220.

2.6 | Preparation of UPRs

Different amounts of DPET, according to Table 1, were dissolved in the commercial liquid UPR via vigorous stirring at room temperature for 1–1.5 h until homogeneous mixtures were obtained. Next, 2% BPO was added to these mixtures and the stirring was continued for about another 30 min. The mixtures were degassed in a vacuum oven. Finally, mixtures were poured into silicone molds and cured at 80°C for 1 h and at 120°C for 3 h.

3 | RESULTS AND DISCUSSION

3.1 | Characterization of DPET

A new DOPO-containing reactive FR having piperazine and triazole rings was aimed. We designed this FR monomer for UPRs in the light of the previous works that state bi-DOPO structure[42] and P–N synergism[12,13,15,45] are beneficial. The novel FR, namely DPET (short for bis-DOPO

TABLE 1 Composition of the unsaturated polyester resins (UPRs).

	UPR (g)	DPET (g)	BPO (g)	P (%)	N (%)	Gel content (%)	Appearance of the UPRs
UPR0	9.8	0	0.2	0	0	97.5	Transparent
UPR5	9.3	0.5	0.2	0.264	0.4775	94	Yellow
UPR10	8.8	1	0.2	0.528	0.955	91.5	Yellow
UPR15	8.3	1.5	0.2	0.792	1.4325	89	Yellow

SCHEME 1 The synthetic route to DPET. [Color figure can be viewed at wileyonlinelibrary.com]

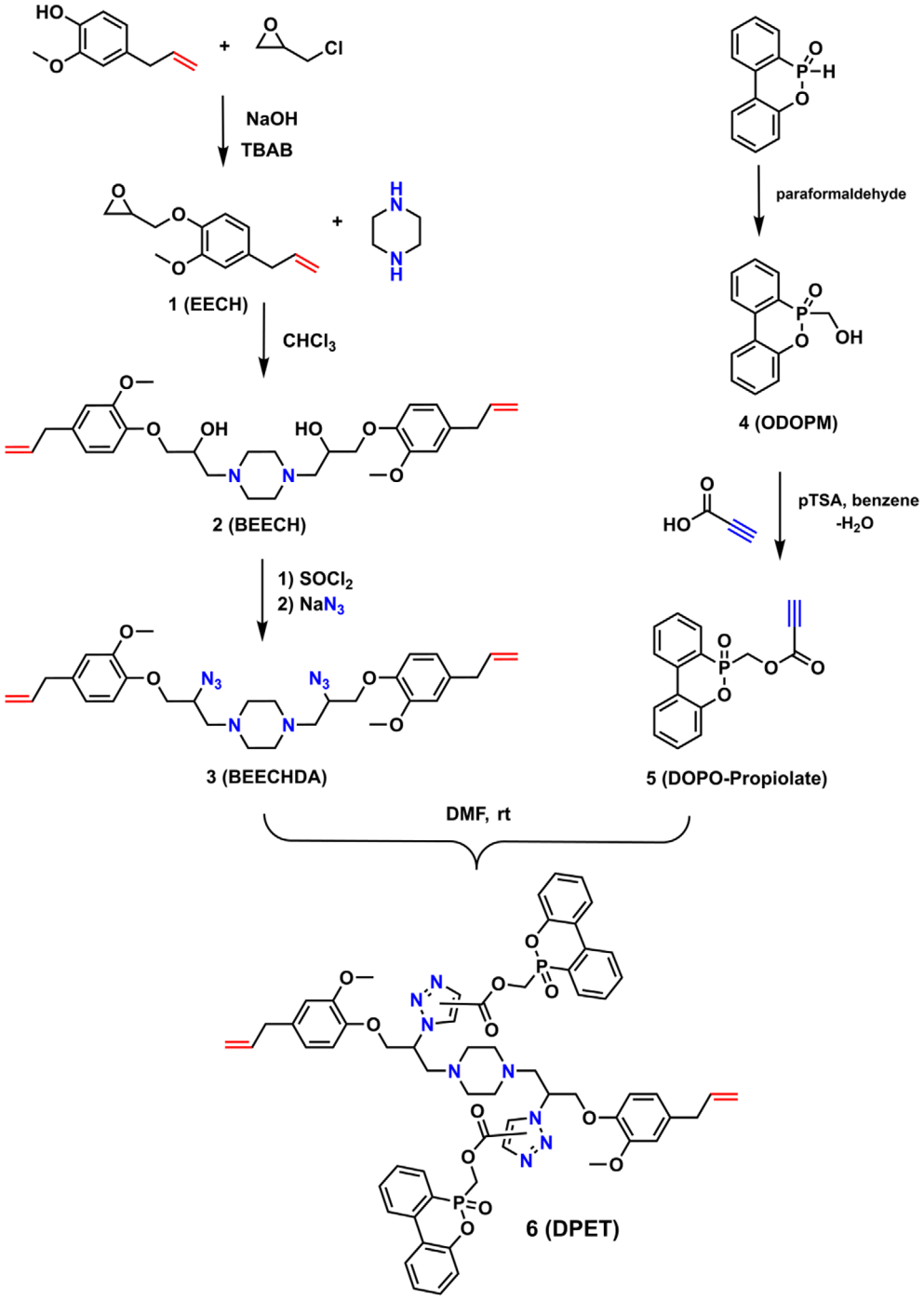

piperazine diallyl bis-triazole), was synthesized in multiple steps, as illustrated in Scheme 1. First, 2 was prepared according to the literature.[37] Next, the hydroxyl groups of 2 were replaced with Cl groups, followed by the azidation reaction to synthesize 3. Finally, 3 and 5 were coupled via a metal-free azide-alkyne click reaction to produce

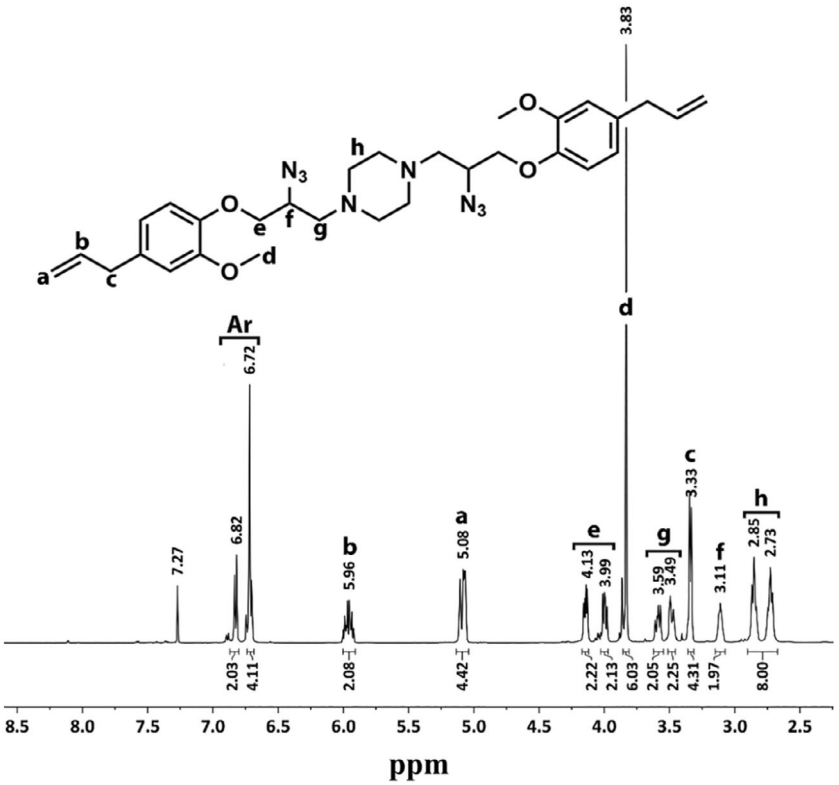

FIGURE 1 Proton nuclear magnetic resonance spectrum of 3.

DPET, which was characterized by FTIR and NMR spectroscopic techniques.

The H-NMR spectrum of 3 is presented in Figure 1. When compared to the NMR spectrum of 2 (see Ref. 36), the hydrogens marked as "g" in 3 were shifted to the downfield region and resonated at around 3.50 ppm. Another significant change in the spectrum of 3 was the shift of the hydrogen marked as "f" to the upfield region due to the shielding effect of the azide groups. The "f" hydrogens were observed at 3.11 ppm. Aromatic hydrogens were found to resonate between 7.0–6.5 ppm while the allyl double bond signals were observed at 5.96 ppm and 5.08 ppm. Other hydrogens marked in Figure 1 fit the structure of 3. The C-NMR given in Figure S1 is in good accordance with the structure of 3 and further confirms its purity. DPET was synthesized from the reaction of 3 and 5, and 5 was prepared from the reaction of propiolic acid and 4. The H-NMR spectrum of 4 is given in Figure S2. The hydrogens of the phenanthrene ring of 4 were observed between 7.26–8.04 ppm. The signals at 4.27–4.07 ppm were assigned to the hydrogens on the carbon atom adjacent to the P atom (–PCH_2OH). In addition to these findings, the absence of the —P—H signal at 8.8 ppm indicates that 4 was synthesized successfully.[50–52] After reacting 4 with propiolic acid, an additional signal was observed (Figure S3) at 2.82 ppm belonging to the hydrogen attached to the terminal carbon atom of the triple bond. Its structure was also confirmed via C-NMR (Figure S4) and P-NMR (Figure S5).

In the final step, 3 and 5 were reacted via metal-free azide–alkyne click reaction to give DPET. The H-NMR spectrum of DPET is given in Figure 2. The hydrogens (k) in the newly formed triazole rings and the aromatic hydrogens belonging to DOPO were found to resonate between 8.00–7.00 ppm and the other aromatic hydrogens (hydrogens in eugenol) were detected at 6.79 and 6.74 ppm. The signals at 5.95 and 5.08 were assigned to the allylic hydrogens of DPET.[36,37] All other hydrogens are marked in Figure 2, and their integral ratios were found to be in good agreement. The structure of DPET was further confirmed via C-NMR (Figure S6).

The structures of all the monomers were also characterized via FTIR spectroscopy. Figure S7. The characteristic azide stretching vibration band of 3 and the —C≡C— stretching band of 5 were observed at around 2100 cm^{-1}. The absence of these bands after the metal-free click reaction proved that the reaction was successful. The FTIR spectrum of DPET also displays the carbonyl vibration band of the propiolate ester group at around 1720 cm^{-1}.

3.2 | Structural characterization of the UPRs

The UPRs were structurally characterized via FTIR spectroscopy (Figure S8). Uncured liquid UPR precursor displayed the characteristic carbonyl stretching vibration

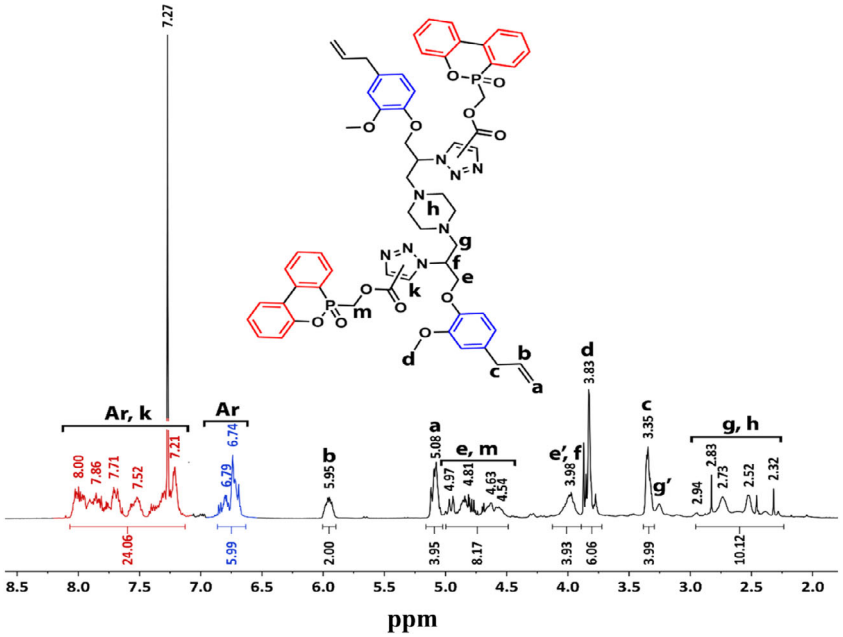

FIGURE 2 Proton nuclear magnetic resonance spectrum of DPET. [Color figure can be viewed at wileyonlinelibrary.com]

band at 1720 cm^{-1}. The bands belonging to the aromatic C—H bonds were observed at around 3050 and 1600 cm^{-1}. The aliphatic —CH_2— and —CH_3 stretching vibration bands were detected at around 2950–2850 cm^{-1}. The double bond vibration bands arising from the maleate and styrene groups were observed at around 1650–1640 cm^{-1}. After curing, the FTIR spectra of the UPRs did not alter much. The intensity of the double bond bands was decreased to some extent indicating the presence of unreacted monomers/oligomers. Additionally, a new band at around 920 cm^{-1} was observed in the spectra of the DPET-containing UPRs, which was attributed to the P—O—C band in DOPO.[38]

The FTIR results indicated that the cured films had unreacted monomers. Therefore, we investigated the degree of curing by measuring the gel content values of the UPRs. The gel content values of the UPRs are listed in Table 1. The gel content values of the UPRs were found to change between 97.5% and 89%. The gel content values were found to decrease with increasing amounts of DPET, yet the decrease was not higher than the added amount of DPET, which indicates that DPET was covalently attached to the polymer matrix. In a previous study, it was reported that the gel content of UPRs containing reactive FR was between 85% and 90%.[27] In another study, an increase in the gel content (77%) of the UPR containing a reactive FR compared to the gel content (69%) of the same UPR containing a similar but unreactive FR.[42] When compared to these previous works, it can be concluded that the UPRs prepared herein have excellent degrees of crosslinking.

3.3 | Water contact angle values of the UPRs

We evaluated the surface wettability of the UPRs by measuring the water contact angle (WCA) values. Since UPRs are generally used in glass fiber-based composites, the wettability of the UPR is important for good adhesion. The WCA values of the UPRs are shown in Figure 3. The neat UPR displayed a WCA of 70°. The WCA values of the UPRs declined slightly with increasing amounts of DPET. This decrease was attributed to the presence of polar substituents such as nitrogen-containing rings and polar —P═O groups. Thus, it can be concluded that the incorporation of DPET in UPRs leads to more hydrophilic surfaces.

3.4 | Optical properties of the UPRs

We measured the light transmittance percentages of the prepared UPR films in the range of 850–250 nm (Figure 4). The pristine UPR films (UPR0) were transparent whereas the DPET-containing UPRs were yellow. As can be seen from Figure 5, the presence of DPET led to a dramatic decrease in the light transmission of the UPRs. DPET contains aromatic rings as well as triazole and eugenol groups, all of which lead to visible light absorption and a corresponding reduction of light transmission. Similar to our findings, it was shown in the literature that thermosets containing a DOPO-based reactive FR reduce visible light transmittance.[41]

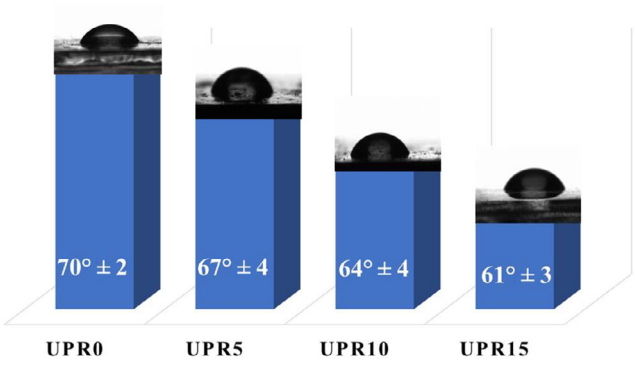

FIGURE 3 WCA values of the unsaturated polyester resins (UPRs). [Color figure can be viewed at wileyonlinelibrary.com]

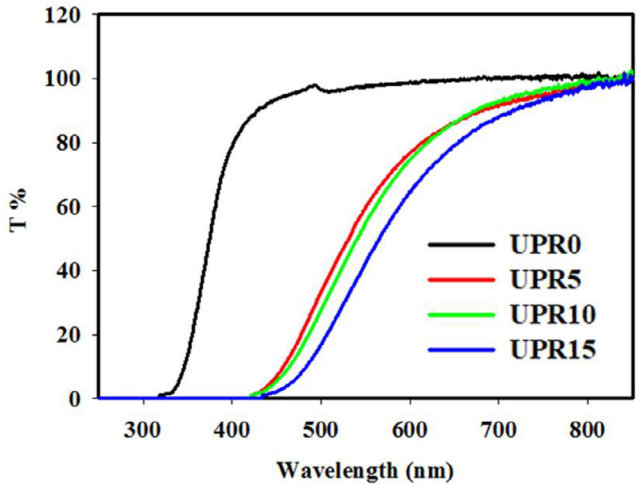

FIGURE 4 UV–Vis transmittance values of the UPRs. [Color figure can be viewed at wileyonlinelibrary.com]

3.5 | Mechanical properties

Often the FRs lead to a decrease in the mechanical properties of polymers. This general case is also valid for UPRs. For instance, Chu et al. reported the synthesis of DOPO-containing polymeric FRs for UPRs.[53] When these polymeric FRs were used in UPRs, tensile strength values declined. In another study, Li et al. prepared a P- and Ni-containing non-reactive FR and this FR led to slightly reduced tensile strength and modulus values.[54] However, when reactive FRs were used, improvements were reported in the mechanical properties.[23,26,27]

The modulus, tensile strength, and the elongation at break values of the UPRs are plotted in Figure 5. As can be seen in this figure, the modulus and the tensile strength of the UPRs increased with increasing amounts of DPET while the elongation at break values decreased gradually. DPET is a rigid molecule with aromatic and triazole rings and large bi-DOPO structures. Also, it is a difunctional monomer that brings additional crosslinking sites to the UPR. Thus, the mechanical properties were enhanced, but it should also be noted that the films became more brittle.

3.6 | Thermal properties of the UPRs

Thermal properties of the prepared UPRs were investigated using TGA and differential scanning calorimetry (DSC) techniques. TGA thermograms of the UPRs are presented in Figure 6, along with the derivative weight curves, and the results obtained are given in Table 2. As can be seen from the TGA thermograms, all UPRs displayed similar two-stage degradation profiles. The first degradation step was attributed to the decomposition of the polystyrene chain within the network, and the second step was attributed to the decomposition of the main polyester chains. The T_1 and T_2 maximum weight loss temperatures were found to be 388°C and 409°C, respectively. The T_1 and T_2 temperatures slightly shifted to lower temperatures as the percentage of DPET was increased in the UPRs. This situation was attributed to the early decomposition of DPET. Generally, phosphorous FRs start to decompose before the main polymer chains, leading to the formation of phosphoric acid species that catalyze the formation of a char residue. In some cases, some radical species are also generated upon decomposition and act in the gas phase. The UPR0, the neat resin, produced 5.6% char at 600°C under N_2 atmosphere. The char yield of the DPET-containing UPRs increased gradually and reached 16.6% when the concentration of DPET was 15% (UPR15).

The glass transition temperatures (T_gs) of the neat UPR and the DPET-containing UPRs were measured via DSC. The DSC thermograms of the UPRs are given in Figure S9 and the T_gs are listed in Table 2. The T_g of the neat UPR was found to be 101.5°C. The T_gs of the DPET-containing UPRs were increased with increasing amounts of DPET. DPET has two allyl groups and contributes to the crosslinking density. Besides, it is a rigid molecule having polar nitrogen-containing rings, and polar —C═O and —P═O groups. The increased T_g values can be attributed to the reduced mobility of the polymer chains as a result of the increased extent of crosslinking and the rigidity of DPET, leading to a significant decrease in the free volume of the polymer matrix. Due to the reactive nature of DPET and its contribution to crosslinking, one would expect a higher increase in the T_g values. The reason for the lower T_g values than expected can be ascribed to the relatively small decrement in the degree of curing (see gel content values).

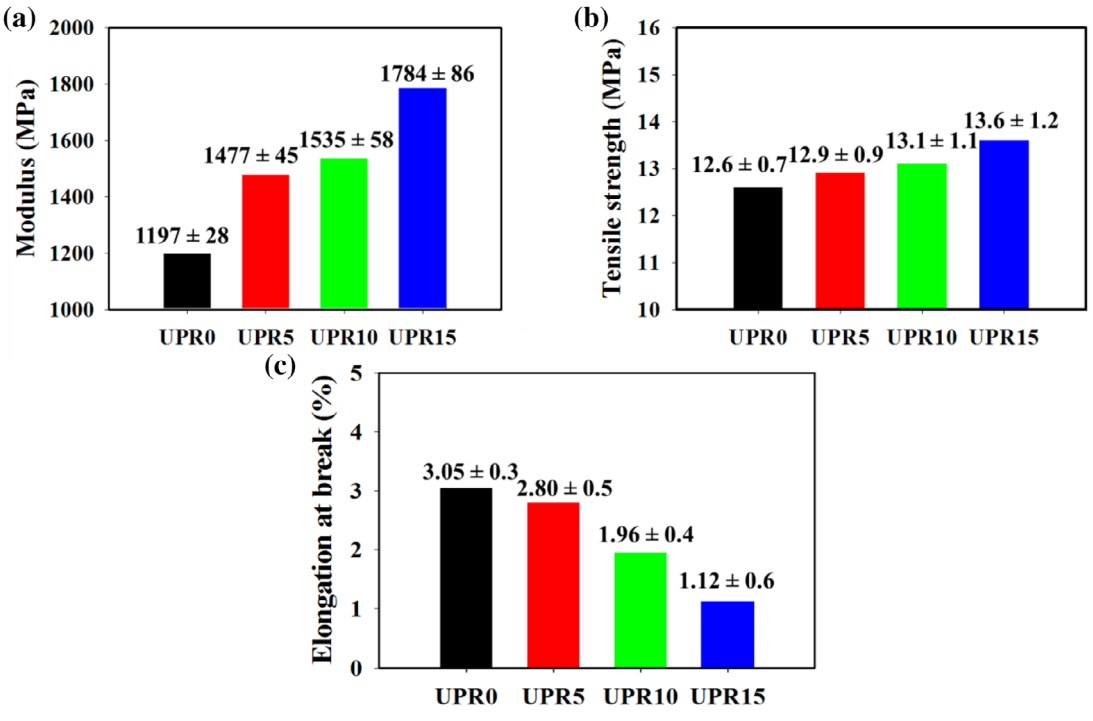

FIGURE 5 Modulus (a), tensile strength (b), and the elongation at break (c) values of the UPRs. [Color figure can be viewed at wileyonlinelibrary.com]

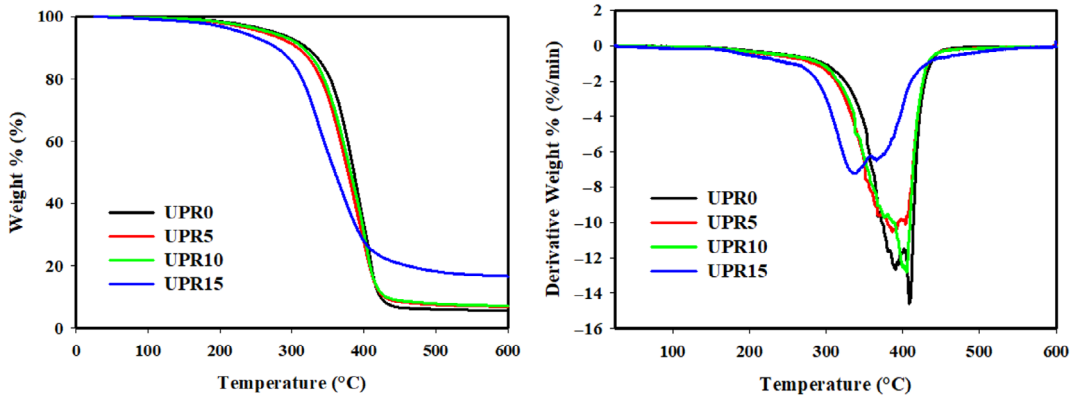

FIGURE 6 Thermogravimetric analyses thermograms and the corresponding derivative weight curves of the unsaturated polyester resins (UPRs). [Color figure can be viewed at wileyonlinelibrary.com]

TABLE 2 Thermal properties of the unsaturated polyester resins (UPRs).

	T_1[a] (°C)	T_2[a] (°C)	Char (%)	T_g[b] (°C)	LOI	UL-94
UPR0	388	409	5.6	101.5	19.0	NR
UPR5	385	404	6.8	105.3	19.8	NR
UPR10	374	402	7.1	106.5	21.2	NR
UPR15	337	365	16.6	111.5	23.4	V1

[a]T1 and T2 are the maximum weight loss temperatures, which were determined from the maximum of the corresponding derivative curves.
[b]Determined by DSC.

3.7 | Flame retardancy of the UPRs

The flame retardancy of the UPRs was assessed by measuring the LOI values and UL-94 ratings. Also, the MCC test was conducted for further evaluation. The LOI values and the UL-94 test ratings of the UPRs are listed in Table 2. The LOI value of the neat UPR (UPR0) was found to be 19.0%. Different LOI values were reported in

the literature for pristine UPRs, which might be due to the use of different grades of UPRs having various chemical compositions, styrene contents, disparate curing methods, and so forth. The LOI values of the UPRs prepared in this work increased when DPET was introduced and continued to increase with its increasing concentration in the polymer matrix. In this study, the highest LOI (23.4%) was measured for the UPR15 encoded samples. Higher LOI values were reported in the literature for UPRs.[25,27,29,41,45] The relatively lower LOI values in this work can be attributed to the high flammability of the neat UPR and the low P percentage in the DPET-containing UPRs. It is clear that to increase the LOI values, the concentration of P had to be increased; however, due to the low solubility of DPET in UPR, we could only add up to 15%. The N content in our designated FR is high, and due to P–N synergism, we expected to reach higher LOI values, yet the high inherent flammability of the neat UPR prevented us from obtaining higher LOI values. This situation is also reflected in the UL-94 test and UPR0, UPR5, and UPR10 encoded samples could not be rated accordingly. Only UPR15, which had a P content of 0.792%, was rated as V1. Wazarkar et al. reported that the UPRs containing 0.73% P have a V1 rating.[27] A survey of the literature showed that in most cases, the P percentage within the UPR should be over 1.4% to achieve a V0 rating in the UL-94 test.

The heat release of UPR samples was evaluated by MCC which measures the total fuel value of a material,[55] to investigate the inherent flammability of UPR resin. The MCC test is a useful tool for evaluating the flame retardancy of products.[56]

Figure 7 displays the HRR versus temperature curves of the UPRs and the MCC test results as the THR, HRC, peak heat release rate (pHRR), the temperature of heat release peak (TPHRR), and the time to attain the heat release peak are listed in Table 3. The digital images of the samples before and after the MCC test are given in Figure S10. As can be seen from these images, the samples containing DPET display much denser black residues compared to neat UPR. Furthermore, the obtained chars for the DPET-containing samples have a foam-like appearance due to the intumescent characteristic of the synthesized FR.

According to the MCC results, the incorporation of DPET has a negligible effect on the TPHRR values. The time to attain the heat release peak for UPR0 was measured as 351 s. This value first decreased when 5% and 10% DPET was added and it slightly increased with further DPET addition. It was found that the pHRRs of the resins were reduced when DPET was incorporated into the UPR matrix. Thus, the potential fire hazard of UPR resin was reduced as less heat was released. As is shown

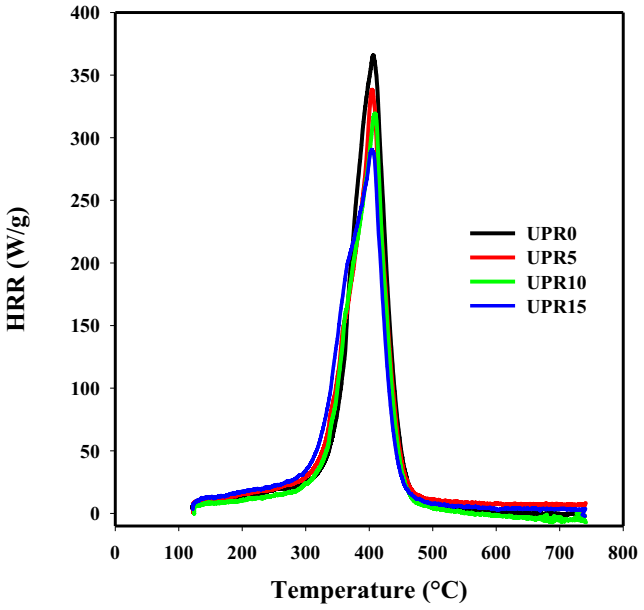

FIGURE 7 HRR curves of the UPRs. HRR, heat release rate; UPRs, unsaturated polyester resins. [Color figure can be viewed at wileyonlinelibrary.com]

in Table 3, the PHRR value of UPR resin incorporated DPET was much lower than that of the neat UPR. Meanwhile, higher DPET content resulted in lower PHRR values, which indicates that the addition of DPET was conducive to improving the fire behavior of the UPR resin. This improvement is associated with the formation of phosphorus-containing radicals like PO• radicals and their effect on the thermal decomposition mechanism of UPR resin. The phosphorus-containing groups in DPET were thermally decomposed to form PO• radicals. The PO• radical entering the gas phase can eliminate the volatile organic compounds generated in combustion, thus inhibiting the further decomposition of the UPR resin.[57] These MCC data clearly demonstrate that the incorporation of DPET could improve the flame resistance of the UPR resin.

Neat UPR displayed a pHRR value of 351 W/g, indicating that it is highly combustible. With the introduction of DPET, the PHRR values started to shift to lower values, indicating improved flame resistance. When only 5% of DPET was introduced pHRR value decreased to 329 W/g. When the ratio of DPET was increased to 15%, the pHRR value further decreased to 257 W/g, resulting in a ∼ 27% reduction in the pHRR. Similarly, both the HRC and THR values gradually decreased with increasing amounts of DPET. It must be noted here that better results were reported in the literature.[23,40,41,42] For instance, according to the MCC test results, the reactive FR called ODOPB-AC led to a 30% decline in the pHRR values when used at a ratio of 20%.[40] In another study,

TABLE 3 MCC data of the UPRs.

	THR (kJ/g)	HRC (J/g K)	pHRR (W/g)	TPHRR (°C)	Time (s)
UPR0	30.1	387	351	401	351
UPR5	27.9	370	329	403	342
UPR10	24.9	344	292	400	341
UPR15	22.2	305	257	399	344

Abbreviations: HRC, heat release capacity; MCC, micro cone calorimeter; THR, total heat release; Time: the time to attain the heat release peak; TPHRR, temperature of heat release peak; pHRR, peak heat release rate.

when 20% of the reactive FR (DHP) synthesized by Lin et al. was incorporated into a UPR, the pHRR value was decreased by 37.2%.[41] On the other hand, when the DHP's concentration was 15%, the reduction in pHRR was about 28%. The relatively lower values reported herein can be attributed to the low percentage of the newly synthesized FR in the prepared UPRs and hence the low amount of P content.

3.8 | TGA–FTIR test

Simultaneous TGA–FTIR analysis is used to determine the decomposition profile of polymer matrixes. In the simultaneous TGA–FTIR test, its weight loss is deliberated when the polymer is heated by TGA while the evolved gases are analyzed by FTIR to identify the chemical species released during decomposition at the same time. The results of simultaneous TGA–FTIR analysis were given in Figure 8 to comprehend the decay process of prepared UPRs at the temperatures resulting in max weight loss and HRR. The evolved gas products of the UPRs were identified at different temperatures illustrated in Figure S11.

The gas phase flame retardancy of P containing UPR is understood by correlating the weight loss data from TGA with the gas release detected by FTIR during thermal degradation. The gaseous products of polymers were characterized by absorptions at 1580 and 1236 cm^{-1} (aromatics), 2347 and 2310 cm^{-1} (CO_2), 3070 and 2968 cm^{-1} (hydrocarbons especially VOCs), and 3730 cm^{-1} (phenols). Figure S11 shows that CO_2 (2347 and 2310 cm^{-1}), VOCs (3070 and 2968 cm^{-1}), and phenols (3730 cm^{-1}) were reduced by the increasing P content. In UPR15, 2347 and 2310 cm^{-1} peaks disappeared because of small CO_2 release lower than atmospheric CO_2 level. It was recommended that the peaks at 1234 cm^{-1} (P═O), 750 cm^{-1} (P—O—C), and 1007 cm^{-1} (P—O—Ph) were decay products of UPRs containing P-referring phosphate ester fragments. The other major peaks are shown in the 1500 and 1600 cm^{-1} (NO) and 1500 and 1600 cm^{-1} (NO_2) related to N content of UPR_S and inert atmosphere used in the TGA–FTIR test.[53,58,59]

3.9 | Morphologies of the char residues

The microstructure of the char residues of UPR0 and UPR15 were investigated by SEM–EDX. The scanning electron microscopy (SEM) micrographs of UPR0 and UPR15 at different magnifications are presented in Figure 9. The micrographs of the char residues exhibit interpenetrating carbonaceous networks with porous surface morphology. As can be seen from Figure 9, the char residue of UPR15 is much more compact and less porous. There are more open-holes in UPR0 compared to UPR15, which leads to reduced barrier properties.

Representative energy dispersive X-ray (EDX) spectra of UPR0 and UPR15 are given in Figure S12. According to the EDX results the char residue of UPR0 is composed of mostly carbon (92.96%). The introduction of DPET led to the reduction of the carbon content to 87.81% and the P content on the surface of the char residue of UPR15 was measured as 3.95%. This high amount of P on the surface of UPR15 indicates a good level of condensed phase action of the DPET. Thus, the improved flame retardancy of UPR15 can be attributed to the formation of the phosphorous-rich carbonaceous char. We further evaluated the char residues via FTIR spectroscopy. As can be seen from Figure S13, the intensities of the vibrations of the carbonyl and aromatic double bonds in neat UPR (UPR0) are reduced, indicating that most of the constituents of the UPR are decomposed. On the other hand, the presence of DPET protected and delayed the burning of neat UPR as evident from the FTIR spectrum of the char residue of UPR15 (Figure S13) which displays —P═O, —P—O—C, and —P—O—P— vibration bands at 1114, 1034, and 990 cm^{-1}, respectively.[60–62]

3.10 | Comparison of the result with the literature

Even though the findings of this paper are compared to the literature in the sections above, for a final and overall assessment of the flame retardancy performance of DPET, we collected and tabulated several data (LOI, UL-94, MCC, TGA, etc) of reactive group-containing FRs

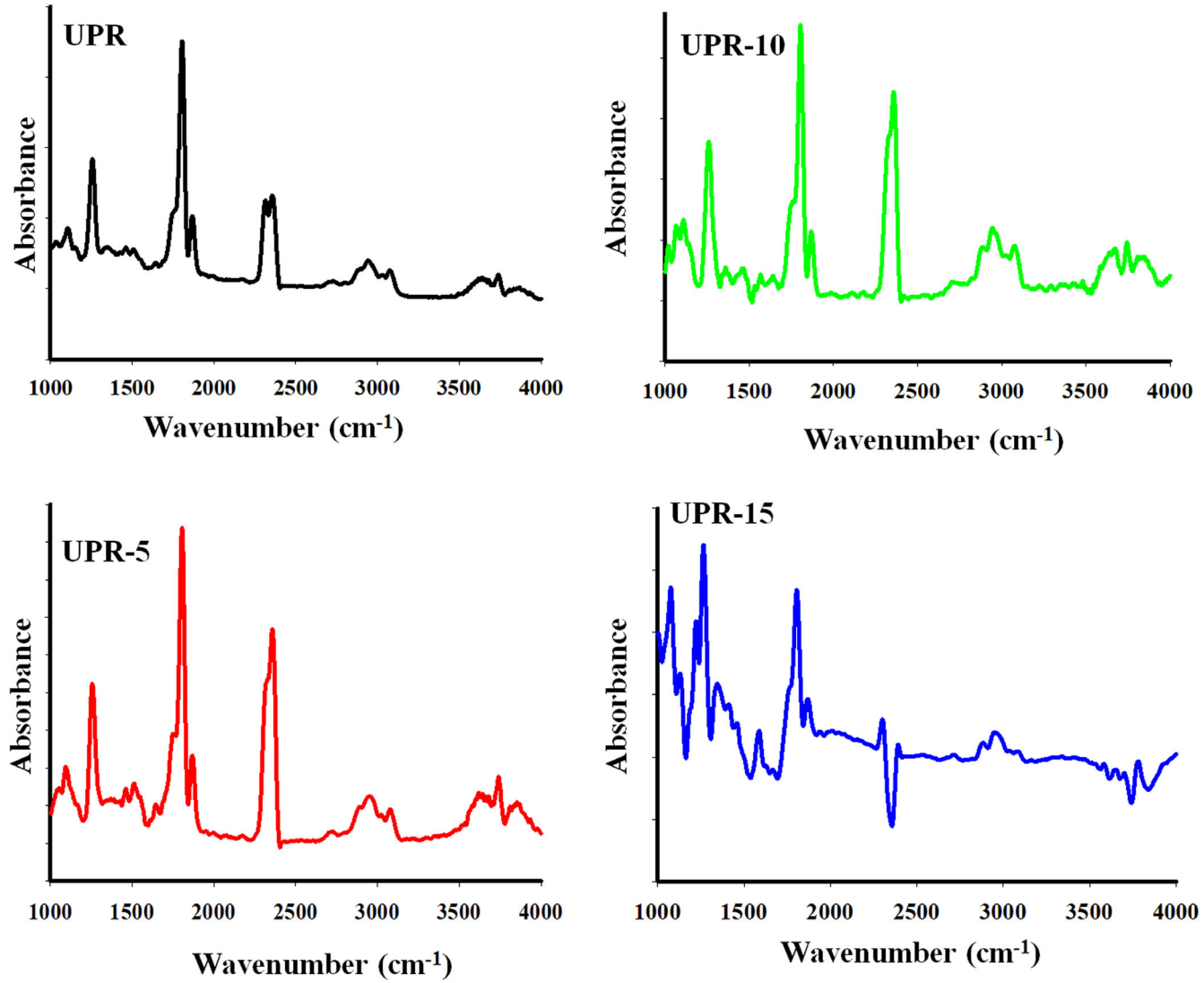

FIGURE 8 Results of simultaneous TGA–FTIR test for unsaturated polyester resins (UPRs). [Color figure can be viewed at wileyonlinelibrary.com]

designed for UPRs (Table S1). It can be seen from Table S1 that DPET is the second lowest P-containing FR. TGIC–AA–DOPO which has the lowest P%, requires to be added at a weight ratio of 40% to achieve a V0 rating in the UL-94 test. Moreover, this Table shows the importance of the initial LOI value of the neat UPR. In our case, the LOI value of our pristine UPR was 19.0%, therefore it is highly flammable. As can be seen from Table S1, there are neat UPRs that display inherently much higher LOI values such as 22.0% or 23.0% and in these cases, it would be much easier to increase the LOI value to higher values compared to a UPR resin exhibiting relatively higher flammability as it is in our case.

Another thing that must be noted here is that DPET has a remarkable performance in terms of TGA. Even though DPET has less P% than ODOBP-AC, the TGA (Note that the heating rates in these two studies (this work and Ref. 40) are different) of 15% DPET-containing UPR led to a 16% char yield at 600°C under nitrogen atmosphere whereas 20% ODOBP-AC-containing UPR produced a much lower char yield (6.41%). This shows that the presence of N-containing rings in DPET leads to a synergistic effect and produces large amounts of char. Nevertheless, according to Table S1, it is clear that the P % needs to be higher in the FR-containing UPR resin and the FR percentage should be at least 20% to be rated V0 in the UL-94 test. Since we were able to dissolve only up to 15% of DPET in the UPR, DPET-containing UPRs reached to V1 rating but failed to reach to V0 rating and higher LOI values.

4 | CONCLUSIONS

Herein, a novel triazole- and piperazine-containing reactive FR (DPET) for UPRs was synthesized. A metal-free

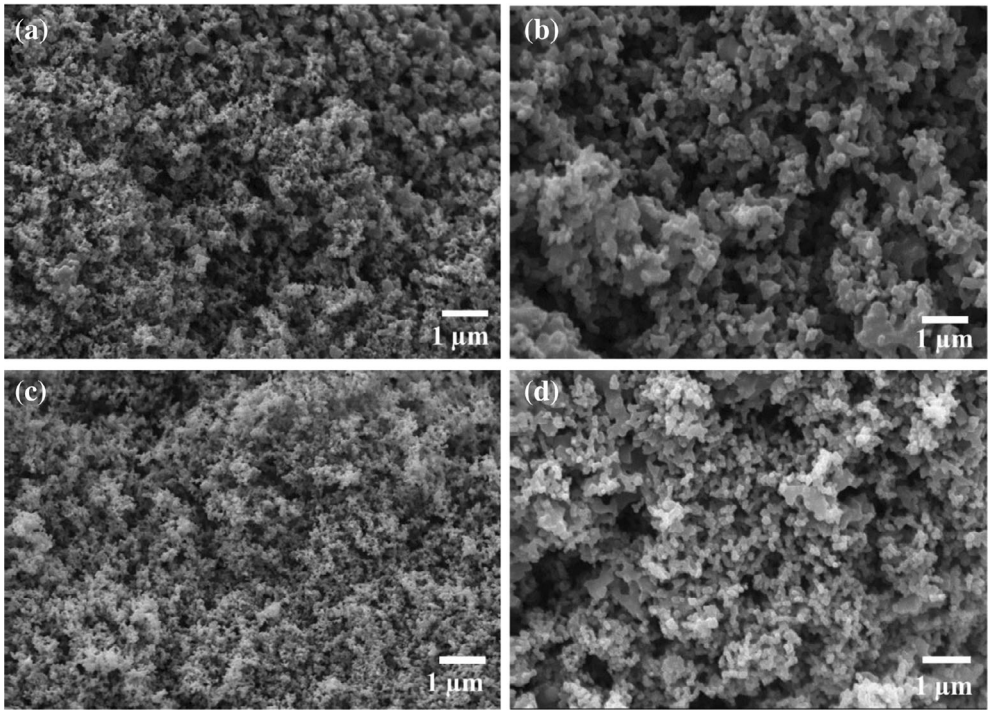

FIGURE 9 SEM micrographs of UPR0 (a, b) and UPR15 (c, d).

azide-alkyne click reaction was utilized for the first time to synthesize a reactive FR for UPRs.

The gel content values of the UPRs were found to change between 97.5%–89%. DPET was added to a neat UPR of up to 15%. The addition of DPET to UPR led to improved hydrophilicity, thermal properties, and flame retardancy. The addition of 15% of DPET into neat UPR led to a water contact angle of 61° ± 2. The char yield at 600°C under a nitrogen atmosphere was increased to 16.6% (15% DPET-containing UPR) from 5.6% (neat UPR). The modulus of the 15% of DPET-containing UPR was measured to be 1784 ± 86 MPa and the LOI value of this composition was found as 23.4%. According to the MCC test, the addition of DPET leads to a reduction in pHRR values. Yet, none of the prepared DPET-containing resins passed the UL-94 test, which was attributed to the low amount of P within the DPET-containing UPRs. However, to reach better UL-94 ratings, DPET can be combined with commercial high FR having more P%, such as APP or dimethyl methylphosphonate, etc.

Nevertheless, this study is an intriguing example of a novel FR, demonstrating the combination of a phosphorus building block; DOPO, with two widely utilized N-containing rings; triazole and piperazine, in a single reactive FR monomer by using a modern synthetic pathway; metal-free azide-alkyne click chemistry. To our knowledge, this is the first example of an FR compound that links triazole and piperazine groups by the use of a metal-free click reaction. We believe this work offers a unique and fresh perspective on the synthesis and design of FRs. With further improvements, the materials prepared herein can be used in buildings, automotive, and glass fiber composites.

In upcoming investigations, our studies will focus on the development of FRs that have enhanced P percentages. Additionally, we will keep working on the synthesis of FRs comprising both P and N elements, employing contemporary click chemistry methodologies.

AUTHOR CONTRIBUTIONS

Ozge Ozukanar: Investigation (lead). **Gokhan Sagdic:** Investigation (equal). **Emrah Çakmakçı:** Investigation (equal); writing – original draft (lead). **Fadime Karaer Özmen:** Investigation (equal); writing – original draft (equal). **Mustafa E. Üreyen:** Investigation (equal); writing – original draft (equal). **Ufuk Saim Gunay:** Writing – review and editing (equal). **Hakan Durmaz:** Writing – review and editing (lead). **Volkan Kumbaraci:** Conceptualization (lead); funding acquisition (lead); investigation (equal); writing – original draft (equal).

ACKNOWLEDGMENTS

This work was supported by the Scientific Research Projects Department of Istanbul Technical University (ITU-BAP).

CONFLICT OF INTEREST STATEMENT

The authors declare no conflicts of interest.

DATA AVAILABILITY STATEMENT

The data that support the findings of this study are available from the corresponding author upon reasonable request.

ORCID

Emrah Çakmakçı https://orcid.org/0000-0002-2876-7460

REFERENCES

[1] E. Çakmakçi, *Polyhedral Oligomeric Silsesquioxane (POSS) Polymer Nanocomposites*, Elsevier, Amsterdam, Netherlands **2021**, p. 127.

[2] J. Cai, H.-M. Heng, X.-P. Hu, Q.-K. Xu, F. Miao, *Polym. Degrad. Stab.* **2016**, *126*, 47.

[3] M. Jiang, Y. Zhang, Y. Yu, Q. Zhang, B. Huang, Z. Chen, T. Chen, J. Jiang, *J. Appl. Polym. Sci.* **2018**, *136*, 47180.

[4] M. Gao, H. Wang, Y. Wang, T. Shen, W. Wu, *J. Vinyl Addit. Technol.* **2014**, *22*, 350.

[5] Z. Bai, S. Jiang, G. Tang, Y. Hu, L. Song, R. K. K. Yuen, *Polym. Adv. Technol.* **2013**, *25*, 223.

[6] J. Zhang, Y. Fang, A. Zhang, Y. Yu, L. Liu, S. Huo, X. Zeng, H. Peng, P. Song, *Prog. Org. Coat.* **2023**, *185*, 107910.

[7] F. Chu, W. Hu, L. Song, Y. Hu, *Fire Technol.* **2024**, *60*, 1077.

[8] F. Chu, S. Qiu, S. Zhang, Z. Xu, Y. Zhou, X. Luo, X. Jiang, L. Song, W. Hu, Y. Hu, *J. Colloid Interface Sci.* **2022**, *608*, 142.

[9] G. Jiang, L. Chen, S. Jiang, K. Zhou, X. Shi, W. Mou, *Adv. Polym. Technol.* **2018**, *37*, 2674.

[10] S. M. Seraji, P. Song, R. J. Varley, S. Bourbigot, D. Voice, H. Wang, *Chem. Eng. J.* **2022**, *430*, 132785.

[11] W.-J. Hu, Y.-M. Li, S.-L. Hu, Y.-R. Li, D.-Y. Wang, *Colloids Surf. A* **2023**, *658*, 130708.

[12] L. Chen, D. Zhao, X.-L. Wang, Y.-Z. Wang, *Chem. Eng. J.* **2022**, *443*, 136365.

[13] S.-L. Hu, Y.-M. Li, W.-J. Hu, J. Hobson, D.-Y. Wang, *Polym. Degrad. Stab.* **2022**, *206*, 110190.

[14] X. Fan, F. Xin, W. Zhang, H. Liu, *React. Funct. Polym.* **2022**, *174*, 105260.

[15] Z. Li, T. Fu, D.-M. Guo, J.-H. Lu, J.-H. He, L. Chen, W.-D. Li, Y.-Z. Wang, *Polymer* **2023**, *275*, 125928.

[16] Z. Bai, L. Song, Y. Hu, X. Gong, R. K. K. Yuen, *J. Anal. Appl. Pyrolysis* **2014**, *105*, 317.

[17] K. Salasinska, M. Celiński, M. Barczewski, M. K. Leszczyński, M. Borucka, P. Kozikowski, *Polym. Test.* **2020**, *84*, 106379.

[18] T. Chu, Y. Lu, B. Hou, P. Jafari, Z. Zhou, H. Peng, S. Huo, P. Song, *Polym. Degrad. Stab.* **2024**, *225*, 110796.

[19] M. Gao, G. Guo, Z. Chai, D. Yi, L. Qian, *Fire Mater.* **2021**, *46*, 743.

[20] M. Gao, Y. Wang, X. Chen, H. Wang, *J. Therm. Anal. Calorim.* **2019**, *138*, 1097.

[21] W. Wang, Y. Peng, H. Chen, Q. Gao, J. Li, W. Zhang, *Polym. Compos.* **2017**, *38*, 2312.

[22] Z. Chen, M. Jiang, Q. Zhang, Y. Yu, G. Sun, J. Jiang, *Int. J. Anal. Charact.* **2017**, *22*, 509.

[23] K. Dai, L. Song, R. K. K. Yuen, S. Jiang, H. Pan, Y. Hu, *Ind. Eng. Chem. Res.* **2012**, *51*, 15918.

[24] K. Dai, L. Song, Y. Hu, *High Perform. Polym.* **2013**, *25*, 938.

[25] K. Dai, L. Song, S. Jiang, B. Yu, W. Yang, R. K. K. Yuen, Y. Hu, *Polym. Degrad. Stab.* **2013**, *98*, 2033.

[26] G. Zhang, D. Song, S. Ma, Y. Wang, X. Xie, Y. Dong, *Polym. Adv. Technol.* **2021**, *32*, 1604.

[27] K. Wazarkar, M. Kathalewar, A. Sabnis, *Polym. Compos.* **2017**, *38*, 1483.

[28] J. Ma, D. Wang, S. Fu, *J. Appl. Polym. Sci.* **2021**, *138*, 50853.

[29] Y. Lin, B. Yu, X. Jin, L. Song, Y. Hu, *RSC Adv.* **2016**, *6*, 49633.

[30] C. A. Wilkie, A. B. Morgan Eds., *Fire retardancy of polymeric materials*, CRC press, Boca Raton **2009**.

[31] A. B. Morgan, J. W. Gilman, *Fire Mater.* **2013**, *37*, 259.

[32] A. Dasari, Z.-Z. Yu, G.-P. Cai, Y.-W. Mai, *Prog. Polym. Sci.* **2013**, *38*, 1357.

[33] E. Cakmakci, M. V. Kahraman, *Photocured Materials*, Vol. 108, The Royal Society of Chemistry, Cambridge, UK **2015**, p. 150.

[34] B. Schartel, *Materials* **2010**, *3*, 4710.

[35] G. Sagdic, E. Cakmakci, O. Daglar, U. S. Gunay, G. Hizal, U. Tunca, H. Durmaz, *Prog. Org. Coat.* **2022**, *167*, 106825.

[36] O. Ozukanar, E. Çakmakçi, O. Daglar, H. Durmaz, V. Kumbaraci, *Eur. Polym. J.* **2023**, *195*, 112203.

[37] O. Ozukanar, E. Çakmakçi, G. Sagdic, U. S. Gunay, H. Durmaz, V. Kumbaraci, *J. Polym. Environ.* **2023**, *31*, 3259.

[38] M. Hamidov, E. Çakmakçi, M. V. Kahraman, *Mater. Chem. Phys.* **2021**, *267*, 124636.

[39] S. Huo, S. Yang, J. Wang, J. Cheng, Q. Zhang, Y. Hu, G. Ding, Q. Zhang, P. Song, H. Wang, *ACS Appl. Polym. Mater.* **2020**, *2*, 3566.

[40] Z. Bai, L. Song, Y. Hu, R. K. K. Yuen, *Ind. Eng. Chem. Res.* **2013**, *52*, 12855.

[41] Y. Lin, S. Jiang, Z. Gui, G. Li, X. Shi, G. Chen, X. Peng, *RSC Adv.* **2016**, *6*, 86632.

[42] Y. Cao, X.-L. Wang, W.-Q. Zhang, X.-W. Yin, Y.-Q. Shi, Y.-Z. Wang, *Ind. Eng. Chem. Res.* **2017**, *56*, 5913.

[43] J. Kuan, K. Lin, *J. Appl. Polym. Sci.* **2004**, *91*, 697.

[44] H. Duan, S. Ji, T. Yin, X. Tao, Y. Chen, H. Ma, *J. Appl. Polym. Sci.* **2019**, *136*, 47997.

[45] S. Huo, J. Wang, S. Yang, H. Cai, B. Zhang, X. Chen, Q. Wu, L. Yang, *Mater. Res. Exp.* **2018**, *5*, 035306.

[46] J. Feng, L. Liu, Y. Zhang, Q. Wang, H. Liang, H. Wang, P. Song, *Exploration* **2023**, *3*, 20220088.

[47] A. Zhang, J. Zhang, L. Liu, J. Dai, X. Lu, S. Huo, M. Hong, X. Liu, M. Lynch, X. Zeng, P. Burey, P. Song, *J. Mater. Sci. Technol.* **2023**, *167*, 82.

[48] O. Ozukanar, E. Cakmakci, O. Daglar, H. Durmaz, V. Kumbaraci, *J. Appl. Polym. Sci.* **2022**, *139*, e52837.

[49] O. Daglar, E. Çakmakçi, U. S. Gunay, G. Hizal, U. Tunca, H. Durmaz, *Macromol. Mater. Eng.* **2021**, *306*, 2100427.

[50] J.-Y. Shieh, C.-S. Wang, *Polymer* **2001**, *42*, 7617.

[51] Y. Wang, Y. Qing, Y. Sun, M. Zhu, S. Dong, *Des. Monomers Polym.* **2020**, *23*, 1.

[52] L. Liu, R. Lv, *e-Polym.* **2019**, *19*, 235.

[53] F. Chu, S. Qiu, Y. Zhou, X. Zhou, W. Cai, Y. Zhu, L. He, L. Song, W. Hu, *Composites Part B* **2022**, *233*, 109647.

[54] Z. Li, T. Fu, J.-H. Lu, J.-H. He, W.-D. Li, B.-W. Liu, L. Chen, Y.-Z. Wang, *Composites Part B* **2022**, *242*, 110032.

[55] P. Wu, Y. Peng, X. Zhang, G. Zhang, J. Ran, M. Xu, *J. Polym. Eng.* **2022**, *42*, 818.

[56] I. C. Çetinkaya, G. Yüksel, C. Macit, M. E. Üreyen, T. Eren, *ACS Appl. Polym. Mater.* **2021**, *3*, 5277.
[57] Y. Sun, Y. Wang, L. Liu, T. Xiao, *Materials* **2020**, *13*, 127.
[58] D. Liu, P. Ji, T. Zhang, J. Lv, Y. Cui, *Polym. Degrad. Stab.* **2021**, *190*, 109629.
[59] X. Qian, Q. Liu, L. Zhang, H. Li, J. Liu, S. Yan, *Polym. Degrad. Stab.* **2022**, *197*, 109852.
[60] J. Li, M. Gao, Y. Zheng, Y. Guan, D. Yi, *Macromol. Mater. Eng.* **2020**, *305*, 2000454.
[61] J. Zhou, M. Xu, X. Zhang, Y. Leng, Y. He, B. Li, *Polym. Adv. Technol.* **2019**, *30*, 1684.
[62] D. Hoang, T. Nguyen, H. An, J. Kim, *Macromol. Res.* **2016**, *24*, 537.

SUPPORTING INFORMATION

Additional supporting information can be found online in the Supporting Information section at the end of this article.

How to cite this article: O. Ozukanar, G. Sagdic, E. Çakmakçı, F. K. Özmen, M. E. Üreyen, U. S. Gunay, H. Durmaz, V. Kumbaraci, *J. Appl. Polym. Sci.* **2024**, e56127. https://doi.org/10.1002/app.56127